Chronic variable stress activates hematopoietic stem cells

Published in final edited form as:
Nat Med. 2014 July ; 20(7): 754–758. doi:10.1038/nm.3589.

Chronic variable stress activates hematopoietic stem cells

Timo Heidt[#1], **Hendrik B. Sager**[#1], **Gabriel Courties**[1], **Partha Dutta**[1], **Yoshiko Iwamoto**[1], **Alex Zaltsman**[1], **Constantin von zur Muhlen**[2], **Christoph Bode**[2], **Gregory L. Fricchione**[3,4], **John Denninger**[3,4], **Charles P. Lin**[1], **Claudio Vinegoni**[1], **Peter Libby**[5], **Filip K. Swirski**[1], **Ralph Weissleder**[1,6], and **Matthias Nahrendorf**[1]

[1]Center for Systems Biology, Massachusetts General Hospital and Harvard Medical School, Simches Research Building, 185 Cambridge St., Boston, MA 02114, USA

[2]Department of Cardiology and Angiology I, University Heart Center, Freiburg, Germany

[3]Division of Psychiatry and Medicine, Massachusetts General Hospital

[4]Benson–Henry Institute for Mind Body Medicine, Massachusetts General Hospital

[5]Cardiovascular Division, Department of Medicine, Brigham and Women's Hospital, Boston, MA, USA

[6]Department of Systems Biology, Harvard Medical School, Boston, MA, USA.

[#] These authors contributed equally to this work.

Abstract

Exposure to psychosocial stress is a risk factor for many diseases, including atherosclerosis[1,2]. While incompletely understood, interaction between the psyche and the immune system provides one potential mechanism linking stress and disease inception and progression. Known crosstalk between the brain and immune system includes the hypothalamic–pituitary–adrenal axis, which centrally drives glucocorticoid production in the adrenal cortex, and the sympathetic–adrenal–medullary axis, which controls stress–induced catecholamine release in support of the fight–or–flight reflex[3,4]. It remains unknown however if chronic stress changes hematopoietic stem cell activity. Here we show that stress increases proliferation of these most primitive progenitors, giving rise to higher levels of disease–promoting inflammatory leukocytes. We found that chronic stress induced monocytosis and neutrophilia in humans. While investigating the source of leukocytosis in mice, we discovered that stress activates upstream hematopoietic stem cells. Sympathetic nerve fibers release surplus noradrenaline, which uses the β_3 adrenergic receptor to signal bone marrow niche cells to decrease CXCL12 levels. Consequently, elevated hematopoietic stem cell proliferation increases output of neutrophils and inflammatory monocytes. When atherosclerosis–prone *ApoE*$^{-/-}$ mice encounter chronic stress, accelerated hematopoiesis promotes

Corresponding author: Matthias Nahrendorf Center for Systems Biology 185 Cambridge Street Boston, MA 02114 Tel: (617) 643–0500 Fax: (617) 643–6133 mnahrendorf@mgh.harvard.edu.

AUTHOR CONTRIBUTIONS T.H. and H.B.S. performed experiments, collected, analyzed and discussed data and contributed to writing the manuscript. G.C., P.D., A.Z., Y.I., G.C., J.D. performed experiments, collected, analyzed and discussed data, C. vzM., C.B., C.L., C.V., P.L., F.K.S. and R.W. conceived experiments and discussed results and strategy. M.N. managed and designed the study and wrote the manuscript, which was revised and approved by all co–authors.

COMPETING FINANCIAL INTERESTS None

plaque features associated with vulnerable lesions that cause myocardial infarction and stroke in humans.

To explore the impact of stress on the human immune system, we analyzed blood samples from 29 medical residents working on a tertiary hospital intensive care unit (ICU), a challenging, fast–paced work environment that frequently includes the responsibility of life–or–death decisions. Compared to off duty, residents working on ICU reported an increased stress perception which we assessed with Cohen's perceived stress scale[5] (Fig. 1a). Visual analog scales[6] documented a higher stress intensity and frequency while working on ICU (Supplementary Fig. 1a). When comparing samples taken during work to samples taken off duty, we observed an increase in blood leukocytes (Fig. 1b), with higher numbers of neutrophils, monocytes and lymphocytes, after one week of intensive care rotation (Supplementary Fig. 1b). Monocytes' relative subset frequency did not change (Supplementary Fig. 1c).

To test the hypothesis that stress–induced leukocytosis results from increased leukocyte production, we exposed mice to chronic variable stressors validated by behavioral neuroscience studies (Supplementary Table 1)[7-9]. Compared to non–stressed controls, stressed mice had increased numbers of leukocytes, neutrophils and monocytes in blood (Fig. 1c), extending our observation in humans. These cells were also more numerous in the mouse bone marrow (Fig. 1d). We next investigated the influence of chronic stress on blood cell production in the bone marrow and detected increased cycling of Lin^- $Sca–1^+$ $ckit^+$ $CD150^+$ $CD48^-$ hematopoietic stem cells[10] (HSC, Fig. 1e), which also incorporated increased amounts of BrdU (Supplementary Fig. 2a). To study quiescence, we pursued a BrdU pulse–chase label retention experiment. BrdU exposure in drinking water for 2 weeks led to >90% labeling of HSC as previously reported[11]. After completion of the labeling phase, mice were stressed for 3 weeks which accelerated HSC BrdU wash–out when compared to stress–free controls (Supplementary Fig. 2b**).** Augmented colony forming capacity of bone marrow harvested from stressed mice reflected increased progenitor proliferation (Fig. 1f). Enhanced proliferation resulted in higher bone marrow numbers of HSC, $Lineage^-$ $Sca–1^+$ $c–kit^+$ progenitors (LSK, Fig. 1g), granulocyte macrophage progenitors (GMP), macrophage dendritic cell progenitors (MDP, Supplementary Fig. 3a) and common lymphoid progenitors (CLP, Supplementary Fig. 3b). While $CD150^+$ $CD48^-$ SLAM staining phenotypically quantitates HSC, only a fraction of the cells in this gate are functional long–term HSC (LT–HSC)[10]. A competitive repopulation assay[12] comparing limiting bone marrow dilutions obtained from stressed and non–stressed donors indicates that the frequency of LT–HSC does not significantly change in stressed mice (Fig. 1h, Supplementary Table 2). When viewed together with the increased bone marrow cellularity in stressed mice (1.64×10^7 versus 2.46×10^7 per femur, $p<0.0001$, $n = 14–18$ mice), stress does neither increase nor exhaust LT–HSC. An unchanged number of LT–HSC in stressed mice is further supported by comparable donor blood chimerism 16 weeks after transfer of 2×10^6 bone marrow cells from either stressed or non–stressed donors with equal numbers of naive competitor cells into lethally irradiated recipients (Fig. 1i). In contrast, infection and interferons increase HSC proliferation while exhausting LT–HSC[13] or impairing their engraftment[14], possibly because these stimuli are more severe than stress. Of note,

interferons were unchanged in the bone marrow of stressed mice (Supplementary Fig. 4a). A 5–Fluoruracil (5–FU) challenge completely abolished stress–induced leukocytosis. Surprisingly, stressed mice had an enhanced leukocyte rebound on day 14 after 5–FU injection, likely due to increased cycling of hematopoietic progenitors (Supplementary Fig. 4b). Serial intravital microscopy[15] in the calvarium of mice that had undergone adoptive transfer of 25,000 DiD–labeled LSK detected accelerated dilution of the membrane dye in mice exposed to 7 days of stress (Fig. 2a), indicating accentuated cell proliferation. Flow cytometry confirmed the accelerated membrane dye dilution after stress exposure (Fig. 2b). Taken together, these data indicate that chronic stress activates HSC, which increase proliferation and differentiate into downstream progenitors.

Noradrenaline is a prototypical stress hormone that also regulates circadian progenitor cell migration[16] and proliferation[17,18]. We wondered if heightened hematopoietic system activity during stress could relate to this catecholamine. Indeed, noradrenaline levels increased in the bone marrow of stressed mice (Fig. 3a). Immunoreactive staining for tyrosine hydroxylase (TH), a rate–limiting enzyme for noradrenaline synthesis[19], rose along blood vessels in the bone marrow (Fig. 3b). Because noradrenaline regulates CXCL12 synthesis[16], this rise led to a sharp decrease in CXCL12 mRNA and protein within whole bone marrow (Fig. 3c,d). Conditional deletion of TH containing cells in crossbred iDTR TH–cre mice[18] preserved CXCL12 levels and blunted the bone marrow's stress response (Supplementary Fig. 5). In the hematopoietic niche, CXCL12 derives from mesenchymal stem cells, osteoblasts and endothelial cells[20-22]. Its primary functions include inhibiting hematopoietic stem and progenitor cell (HSPC) proliferation and migration, and it also retains neutrophils in the bone marrow[23]. CXCL12 deficient mice[24] and mice that lack the chemokine's cognate receptor (CXCR4)[25] show increased HSC cycling and progenitor pool expansion and increased neutrophil release into circulation. Linking the autonomic nervous system and leukocyte trafficking, the β_3 adrenergic receptor expressed on niche cell surfaces regulates CXCL12 release[16]. Among relevant niche cells, mesenchymal stem cells express the highest level of the β_3 receptor (Supplementary Fig. 6). We therefore investigated if chronic stress acts on hematopoiesis via the β_3 adrenergic receptor. Indeed, mice with genetic lack of the receptor displayed protection against stress (Supplementary Fig. 7). Treating stressed mice with the β_3 selective receptor blocker SR 59230A restored CXCL12 mRNA and protein levels (Fig. 3c,d), decreased BrdU incorporation into HSC and reduced HSPC numbers in the bone marrow (Fig. 3e). Consecutively, downstream GMP and MDP numbers fell (Supplementary Fig. 8a), resulting in lower levels of neutrophils and Ly–6C^{high} monocytes in circulation (Fig. 3f). Treatment with a β_2 receptor blocker failed to protect the bone marrow against stress (Supplementary Fig. 8b,c).

Atherosclerosis is a chronic inflammatory disease driven by hyperlipidemia[26-28]. Atherosclerotic plaques consist of cholesterol deposits and a leukocyte infiltrate that is dominated by innate immune cells[29]. Inflammatory monocytes and macrophages may lead to plaque rupture, myocardial infarction and stroke[30,31], and higher blood levels of monocytes and neutrophils correlate with increased mortality[29,32]. Proteases released from inflammatory leukocytes weaken the fibrous cap and favor plaque disruption that permits contact between the plaque's necrotic core and clotting factors in the blood stream, inciting local thrombosis, and thereby jeopardizing oxygen supply to the heart and brain[30,33]. A

number of risk factors contribute to inflammatory complications of atherosclerosis. Chronic stress is well recognized among them[4,34-37]. Yet the mechanisms that link chronic stress to higher cardiovascular event rates are incompletely understood. This study tested the hypothesis that chronic stress acts on the bone marrow via sympathetic nervous system activity by increasing inflammatory leukocyte supply to atherosclerotic lesions. Stress enhanced the hematopoietic system's activity in atherosclerosis–prone *ApoE*$^{-/-}$ mice (Supplementary Fig. 9a,b) while body weight and lipid levels remained unaffected (Supplementary Fig. 9c,d). Plaque protease levels were measured after exposure to 6 weeks of stress. FMT/CT imaging revealed an increase in protease plaque activity in stressed mice (Fig. 4a). Innate immune cells produce most proteases in the plaque[29,30]. Accordingly, we detected higher CD11b^{+} myeloid cell and neutrophil content in plaque by histology (Fig. 4b) and increased numbers of neutrophils, monocytes and macrophages in whole aortae by flow cytometry (Fig. 4c). Neutrophils may aid monocyte entry into plaque[38] but can also themselves have inflammatory functions[39]. The aorta also exhibited an inflammatory cytokine expression profile after stress (Fig. 4d), including increased expression of myeloperoxidase, a pro–oxidant enzyme abundant in neutrophils and inflammatory monocytes. While aortic root plaque size did not change (Supplementary Fig. 10), the inflammatory milieu led to thinner fibrous caps and larger necrotic plaque cores (Fig. 4e), hallmarks of rupture–prone lesions in patients with acute MI or stroke[29,33]. Heightened recruitment of leukocytes into plaques may also result from enhanced action of adhesion molecules; however, mRNA and protein levels, with the exception of E–selectin, were unchanged in stressed *ApoE*$^{-/-}$ mice (Supplementary Fig. 11a,b). When we adoptively transferred equal numbers of GFP^{+} myeloid cells into stressed and non–stressed *ApoE*$^{-/-}$ mice, we detected similar recruitment (Supplementary Fig. 11c). Hypertension, a known risk factor for atherosclerosis, occurred only during stress exposure (Supplementary Fig. 12a) and therefore likely did not dominate the observed disease progression. Blood pressure, cholesterol and corticosterone levels were unchanged in *ApoE*$^{-/-}$ mice that received a β_3 adrenergic receptor blocker (Supplementary Fig. 12b,c); however, this treatment reduced the number of neutrophils, inflammatory monocytes and macrophages in plaque (Supplementary Fig. 13).

In summary, we report a previously unknown mechanism unleashed by chronic stress episodes on hematopoiesis and describe a new axis of interaction between the central nervous system, immunity and atherosclerosis. In mice exposed to stress, increased sympathetic nervous system activity decreased CXCL12 expression in the hematopoietic stem cell niche, accelerated HSC proliferation, and enhanced neutrophil and monocyte production. These mechanisms yielded extensive release of inflammatory leukocytes into circulation and promoted plaque inflammation. Administering a β_3 adrenergic receptor blocker limited disease progression, supporting the notion that sympathetic nervous signaling via this receptor and targeting CXCL12/CXCR4 interaction in the bone marrow should be explored as potential therapeutic avenues.

The preclinical data parallel our observations in ICU residents; however, we interpret this association with care as nature and timing of stress differed. Further, we were unable to investigate HSC activity in stressed humans. Nevertheless, ICU residents were exposed to

chronic rather than acute stress, favoring a long–term increase of leukocyte supply over short–term leukocyte mobilization. Taken together, these data provide new evidence of the hematopoietic system's role in cardiovascular disease[29,40] and elucidate a direct biological link between chronic variable stress and chronic inflammation, a general concept with implications beyond atherosclerosis.

ONLINE METHODS SECTION

Clinical Study

The clinical study titled 'Effects of socioenvironmental stress on the human hematopoietic system' was an open, monocenter, single arm study enrolling medical residents working on the intensive care unit at University Hospital, Freiburg, Germany. This study was registered with the German Registry for Clinical Studies (DRKS00004821) and approved by the Ethics Committee of Albert–Ludwigs–University Freiburg, Germany (No: 52/13). All residents working on ICU were considered eligible to participate in the study. Exclusion criteria were smoking, any acute or chronic illness, regular intake of medication and failure to consent. Twentynine volunteers (23 male, 6 female, mean age 33.7 ± 0.8 years) were enrolled after signing the informed consent form. Residents gave two blood samples (baseline and stress). The off duty sample (baseline) was collected after 10±0.9 consecutive days off duty. The on duty sample (stress) was collected after 7±0.3 consecutive days ICU duty. Participants completed the Perceived Stress Scale 10 item inventory[5] before starting to work on ICU (baseline) as well as after several weeks on duty (stress). Short term perception for stress frequency and intensity was measured with visual analog scales (scale 0–10)[6] which each participant completed at the time of the blood sampling. The mean circadian time difference between the baseline and the stress sample was 20 ± 15.9 minutes. Blood samples were analyzed in a blinded fashion at the routine clinical laboratory of the University Hospital, Freiburg, Germany.

Mice

We used female C57BL/6, UBC–GFP (C57BL/6–Tg(UBC–GFP)30Scha/J), *ApoE*$^{-/-}$ mice (B6.129P2–Apoetm1Unc/J), TH–cre (B6.Cg–Tg(Th–cre)1Tmd/J) and iDTR (C57BL/6–Gt(ROSA)26Sor$^{tm1(HBEGF)Awai}$/J) mice aged 10–12 weeks (Jackson Laboratories, Bar Harbor, ME). *Adrb3*$^{-/-}$ mice were donated by Drs. Paul Frenette (Albert Einstein College of Medicine, New York, NY, USA) and Bradford Lowell (Beth Israel Deaconess Medical Center, Boston, MA, USA). Nestin–GFP mice were a gift from Dr. Grigori Enikolopov (Cold Spring Harbor Laboratory, NY). All procedures were approved by the Subcommittee on Animal Research Care at MGH. For each experiment, age–matched litter mates were randomly allocated to study groups. Animal studies were performed without blinding of the investigator.

Stress procedures

Mice were exposed to socioenvironmental stressors[7-9] for one or three weeks in C57BL/6 or six weeks in *ApoE*$^{-/-}$ mice. Stress procedures were performed between 7 am and 6 pm. The following stressors were applied: *Cage tilt*: The cage was tilted in an 45 degree angle and kept in this position for six hours. *Isolation*: Mice were individually housed in an area one

quarter of the original cage size (12 × 8 cm) for four hours, followed by *Crowding*, during which 10 animals were housed in one cage for two hours. Mice were monitored during the crowding procedure and "fighters" were separated. *Damp bedding*: Water was added to the cage to moisture the bedding without generating large pools. Mice were kept for six hours with damp bedding. *Rapid light–dark changes*: Using an automatic timer the light was switched with an interval of seven minutes for two hours. *Overnight illumination*: Mice were housed in a separate room with illumination from 7 pm to 7 am. All stressors were randomly shuffled in consecutive weeks. Efficacy of the chronic stress procedures was confirmed by measurement of blood corticosterone levels (Supplementary Fig. 12c).

Lethal irradiation

Mice were irradiated using a split dose of 2 × 600 cGy with an interval of 3 hours in between doses. Animals were irradiated 12 hours prior to bone marrow reconstitution.

Bone marrow reconstitution assays

For competitive bone marrow repopulation assays[41] we co–transferred 2×10^6 whole bone marrow cells from CD45.1 mice after three weeks of stress or from non–stressed controls together with equal cell numbers of CD45.2 competitor cells into lethally irradiated Ubc–GFP CD45.2 mice. Engraftment was assessed comparing blood leukocyte chimerism for CD45.1 cells between groups after 2, 3 and 4 months. For limiting dilution experiments[41] donor doses of 1.5×10^4, 6×10^4, 12.5×10^4 and 5×10^5 whole bone marrow cells from CD45.1 mice after three weeks of stress or non–stressed controls were co–transferred with 5×10^5 CD45.2 competitor cells into lethally irradiated CD45.2 recipients. Engraftment was assessed after four months as at least > 0.1% multi–lineage blood chimerism for B–lymphocytes, T–lymphocytes and myeloid lineage derived from donor bone marrow. Poisson's statistic was calculated using L–calc software (Stemcell Technologies) and ELDA software[42]. Bone marrow of two mice was pooled for each cell population.

Treatment with adrenergic receptor antagonists

To inhibit β_3 adrenergic signaling, a specific antagonist for the adrenergic receptor β_3 (SR 59230A, Sigma–Aldrich) was injected at 5 mg/kg i.p. twice per day[43]. For inhibition of β_2 adrenergic signaling, ICI118,551 hydrochloride (Sigma–Aldrich) was injected daily at a dose of 1 mg/kg i.p.[18] for three weeks. The control groups received saline injections.

Depletion of sympathetic nerve fibers

TH–cre were cross–bred with iDTR mice. 10–12 week old female TH–iDTR mice were intraperitoneally injected with 0.1 μg/kg bodyweight diphtheria toxin (DT) on days 0 and day 3 after initiation of stress procedures[18]. Age–matched litter mates (Th–cre, iDTR or WT) which were also stressed and injected with DT served as controls.

5–FU challenge

Non–stressed mice and mice that had been stressed for three weeks were injected intravenously with 150 mg/kg bodyweight 5–FU (Sigma)[44] on day 0. Mice were then followed over the course of 21 days and absolute number of blood leukocytes were

measured after 7, 14 and 21 days. Stress exposure continued for the remaining 3 weeks after 5–FU exposure.

Tissue processing

Flushed bone marrow was passed through a 40μm cell strainer and collected in phosphate–buffered saline (PBS) containing 0.5% bovine serum albumin and 1% fetal bovine serum (FACS buffer). Aortae were excised, minced and digested in collagenase I (450 U/ml), collagenase XI (125 U/ml), DNase I (60 U/ml) and hyaluronidase (60 U/ml) (all Sigma–Aldrich) at 37º C at 750 rpm for 1 hour. For sorting niche cells, bones were harvested from nestin–GFP mice. Bone marrow endothelial cells (EC) and mesenchymal stem cells (MSC) were obtained by flushing out bone marrow which was then digested in 10 mg/ml collagenase type IV (Worthington) and 20 U/ml DNase I (Sigma)[45]. For obtaining bone osteoblastic lineage cells we crushed bones, washed off residual bone marrow cells three times and then digested and incubated the bone fragments[46,47].

Flow cytometry

For myeloid cells, cells were first stained with mouse hematopoietic lineage markers (1:600 dilution for all antibodies) including phycoerythrin (PE) anti–mouse antibodies directed against B220 (BD Bioscience, clone RA3–6B2), CD90 (BD Bioscience, clone 53–2.1), CD49b (BD Bioscience, clone DX5), NK1.1 (BD Bioscience, clone PK136), and Ter–119 (BD Bioscience, clone TER–119). This was followed by a second staining for CD45.2 (BD Bioscience, clone 104, 1:300), CD11b (BD Bioscience, clone M1/70, 1:600), CD115 (eBioscience, clone M1/70, 1:600), Ly–6G (BD Bioscience, clone 1A8, 1:600), CD11c (eBioscience, clone HL3, 1:600), F4/80 (Biolegend, clone BM8, 1:600) and Ly6C (BD Bioscience, clone AL–21, 1:600). Neutrophils were identified as (CD90/B220/CD49b/NK1.1/Ter119)^{low} (CD45.2/CD11b)^{high} CD115^{low} Ly6G^{high} . Monocytes were identified as (CD90/B220/CD49b/NK1.1/Ter119)^{low} CD11b^{high} (F4/80/CD11c)^{low} Ly–6C$^{high/low}$ or (CD45.2/CD11b)^{high} Ly6G^{low} CD115^{high} Ly–6C$^{high/low}$. Macrophages were identified as (CD90/B220/CD49b/NK1.1/Ter119)^{low} CD11b^{high} Ly6C $^{low/int}$ Ly6G^{low} F4/80^{high}. For hematopoietic progenitor staining we first incubated cells with biotin–conjugated anti–mouse antibodies (1:600 dilution for all antibodies) directed against B220 (eBioscience, clone RA3–6B2), CD11b (eBioscience, clone M1/70), CD11c (eBioscience, clone N418), NK1.1 (eBioscience, clone PK136), TER–119 (eBioscience, clone TER–119), Gr–1 (eBioscience, clone RB6–8C5), CD8a (eBioscience, clone 53–6.7), CD4 (eBioscience, clone GK1.5) and IL7Rα (eBioscience, clone A7R34) followed by pacific orange–conjugated streptavidin anti–biotin antibody. Then cells were stained with antibodies directed against c–kit (BD Bioscience, clone 2B8, 1:600), sca–1 (eBioscience, clone D7, 1:600), SLAM markers[10] CD48 (eBioscience, clone HM48–1, 1:300) and CD150 (Biolegend, clone TC15–12F12.2, 1:300), CD34 (BD Bioscience, clone RAM34, 1:100), CD16/32 (BD Bioscience, clone 2.4G2, 1:600) and CD115 (eBioscience, clone AFS98, 1:600). LSK were identified as (B220 CD11b CD11c NK1.1 Ter–119 Ly6G CD8a CD4 IL7Rα)^{low} c–kit^{high} sca–1^{high}. HSC were identified as (B220 CD11b CD11c NK1.1 Ter–119 Ly6G CD8a CD4 IL7Rα)^{low} c–kit^{high} sca–1^{high} CD48^{low} CD150^{high}. GMP were defined as (B220 CD11b CD11c NK1.1 Ter–119 Ly6G CD8a CD4 IL7Rα)^{low} c–kit^{high} sca–1^{low} (CD34/CD16/32)^{high} CD115 $^{int/low}$. MDP were defined as (B220 CD11b CD11c NK1.1 Ter–119 Ly6G CD8a CD4 IL7Rα)^{low}

c–kit$^{int/high}$ sca–1^{low} (CD34/CD16/32)^{high} CD115^{high}. CLP were identified as (B220 CD11b CD11c NK1.1 Ter–119 Ly6G CD8a CD4)^{low} c–kit^{int} sca–1^{int} IL7Rα^{high}. For staining endothelial cells we used ICAM–1 (Biolegend, clone Yn1/1.7.4, 1:300), ICAM–2 (Biolegend, clone 3C4, 1:300), VCAM–1 (Biolegend, clone 429, 1:300), E–Selectin (CD62E) (BD Bioscience, clone 10E9.6, 1:100), P–Selectin (CD62P) (BD Bioscience, clone RB40.34, 1:100), CD31 (Biolegend, clone 390, 1:600), CD107a (LAMP–1) (Biolegend, clone 1D4B, 1:600) and CD45.2 (Biolegend, clone 104, 1:300). Streptavidin–Pacific Orange was used to label biotinylated antibodies. Endothelial cells were identified as CD45.2^{low}, CD31^{high} and CD107a$^{intermed/high}$. For analysis of human monocyte subsets, cells were stained with HLA–DR (Biolegend, clone L243, 1:600), CD16 (Biolegend, clone 3G8, 1:600) and CD14 (Biolegend, clone HCD14, 1:600) after red blood cell lysis (RBC Lysis buffer, Biolegend). Monocytes were identified using forward and side scatter as well as HLA–DR. Within this population, frequencies of monocyte subsets CD14^{high}, CD16^{high} and CD14^{high}/CD16^{high} were quantified.

BrdU experiments

For BrdU pulse experiments we used APC/FITC BrdU flow kits (BD Bioscience). One mg BrdU was injected i.p. 24 hours prior to organ harvest. BrdU staining was performed according to the manufacturer's protocol. For BrdU application over seven days osmotic micro–pumps (Alzet) filled with 18mg BrdU were implanted. For the BrdU label–retaining pulse chase assay, BrdU was added to drinking water (1 mg/ml) for 17 days[11].

Cell cycle analysis

After surface staining, an intracellular staining was performed according to eBioscience's protocol: cells were were fixed and permeabilized using the Foxp3/Transcription Factor Staining Buffer Set (eBioscience) and then stained for the nuclear antigen Ki67 (eBioscience, clone SolA15). The cell cycle was determined using 4,6–diamidino–2–phenylindole (DAPI, FxCycle Violet Stain, Life Technologies).

Cell sorting

To isolate HSPC we used MACS depletion columns (Miltenyi) after incubation with a cocktail of biotin–labeled antibodies (as described in the flow cytometry section) followed by an incubation with streptavidin–coated microbeads (Miltenyi). Then cells were stained with c–kit and sca–1 and LSK were FACS–sorted using a FACSAria II cell sorter (BD Biosystems). To purify niche cells from hematopoietic cells we used MACS depletion columns after incubation with a cocktail of biotin–labeled antibodies as above followed by an incubation with streptavidin–coated microbeads. Then cells were stained with CD45.2, sca–1, CD31 and CD51 (Biolegend, clone RMV–7, 1:100). Endothelial cells were identified as lin^{low} CD45^{low} sca–1^{high} CD31^{high}. Bone marrow MSC were identified as lin^{low} CD45^{low} CD31^{low} sca–1$^{high/intermediate}$ and GFP^{+}. Osteoblasts were lin^{low} CD45^{low} sca–1^{low} CD31^{low} CD51^{high}. For adoptive transfer of GFP^{+} neutrophils and Ly6C^{high} monocytes, bone marrow cells were collected from Ubc–GFP mice for purification of neutrophils and monocytes using MACS depletion columns after incubation with a cocktail of PE–labeled antibodies including B220, CD90, CD49b, NK1.1 and Ter–119 followed by

an incubation with PE–coated microbeads. Aortic endothelial cells were identified as CD45.2^{low} CD31^{high} CD107a$^{int/high}$ and FACS–sorted using a FACSAria II cell sorter.

Adoptive transfer

We injected 2 × 10^6 neutrophils together with 2 × 10^6 Ly6C^{high} monocytes intravenously into non–stressed and stressed *ApoE*$^{-/-}$ mice (stressed for six weeks, cells injected two days prior to the end of these six weeks). Aortae were harvested 48 hours later. The number of CD11b^{high} GFP$^+$ cells within the aorta was quantified by using flow cytometry.

Histology

Aortic roots were harvested and embedded to produce 6μm sections which were stained using an anti–CD11b (BD Biosciences, clone M1/70) or anti–Ly6G (Biolegend, clone 1A8) antibody followed with a biotinylated secondary antibody. For color development we used the VECTA STAIN ABC kit (Vector Laboratories, Inc.) and AEC substrate (DakoCytomation). Necrotic core and fibrous cap thickness were assessed using Masson trichrome (Sigma) staining. Necrotic core was evaluated measuring the total acellular area within each plaque. For fibrous cap thickness three to five measurements representing the thinnest part of the fibrous cap were averaged for each plaque as previously described[48]. For tyrosine hydroxylase staining, femurs were harvested and fixed in 4% paraformaldehyde for 3 hours, then decalcified in 0.375 M EDTA in PBS for 10 days prior to paraffin embedding. Sections were cut and stained with anti–tyrosine hydroxylase antibody (Millipore) after deparaffinization and rehydration. Sections were scanned with NanoZoomer 2.0–RS (Hamamatsu) in 40 × magnification and analyzed using IPLab (Scanalytics).

Intravital microscopy (IVM)

For intravital microscopy of hematopoietic progenitors in the bone marrow of the calvarium, LSK were isolated from either wild type C57BL/6 or C57BL/6–Tg(UBC–GFP)30Scha/J mice and labelled with the lipophilic membrane dye DiD (1,1′–dioctadecyl–3,3,3′,3′–tetramethylindodicarbocyanine perchlorate, Invitrogen). 25,000 labelled LSK were transferred IV into non–irradiated C57BL/6 recipient mice. For blood pool contrast, TRITC–dextran (Sigma) was injected immediately prior to imaging. OsteoSense 750 (PerkinElmer) was injected i.v. 24 hours before *in vivo* imaging to outline bone structures in the calvarium[49]. *In vivo* imaging was performed on days 1 and 7 after the adoptive cell transfer using an IV100 confocal microscope (Olympus)[15]. Three channels were recorded (DiD: excitation/emission 644/665 nm, OsteoSense 750: excitation/emission 750/780 nm, TRITC–Dextran: excitation/emission 557/576 nm) to generate Z–stacks of each location at 2 μm steps. Image post–processing was performed using Image J software. Mean DiD fluorescence intensity was measured for each labelled cell and then normalized to the background by calculating the target to background ratio.

CFU–assay

Colony forming unit (CFU) assays were performed using a semisolid cell culture medium (Methocult M3434, Stem Cell Technology) following the manufacturer's protocol. Bones were flushed with Iscove's Modified Dulbecco's Medium (Lonza) supplemented with 2%

fetal calf serum. 2×10^4 bone marrow cells were plated on a 35 mm plate in duplicates and incubated for 7 days. Colonies were counted using a low magnification inverted microscope.

Blood pressure and heart rate measurement

Blood pressure and heart rate were measured using a non–invasive tail–cuff system (Kent Scientific Corporation) according to the manufacturer's instructions. For each value the mean of three consecutive measurements was used.

Quantitative real–time PCR

Messenger RNA (mRNA) was extracted from aortic arches or bone marrow using the RNeasy Mini Kit (Qiagen) or from FACS–sorted cells using the Arcturus PicoPure RNA Isolation Kit (Applied Biosystems) according to the manufacturers' protocol. One microgram of mRNA was transcribed to complimentary DNA (cDNA) with the high capacity RNA to cDNA kit (Applied Biosystems). We used Taqman primers (Applied Biosystems). Results were expressed by Ct values normalized to the house keeping gene *Gapdh*.

Fluorescence Molecular Tomography–Computed Tomography (FMT/CT)

After six weeks of stress, FMT/CT imaging was performed and compared to non–stressed, age–matched *ApoE*$^{-/-}$ controls. Pan–cathepsin protease sensor (Prosense–680, PerkinElmer, 5 nmol) was injected intravenously 24 hours prior to the imaging as previously described[50].

ELISA

Blood corticosterone levels were measured by ELISA (Abcam). Serum was collected between 10 am and 12 pm. For measurements of noradrenaline in the bone marrow a 2–CAT (A–N) Research ELISA (Labor Diagnostika Nord) was used. One femur was snap–frozen and immediately homogenized in a catecholamine stabilizing solution containing sodium metabisulfite (4 mM), EDTA (1 mM) and hydrochloric acid (0.01 N). Prior to the ELISA the pH of the sample was adjusted to 7.5 using sodium hydroxide (1 N). ELISAs for CXCL12 (R&D), INF–α (PBL Biomedical Laboratories) and INF–γ (R&D) in the bone marrow were performed by using one femur and one tibia per mouse[14]. ELISAs were performed according to the manufacturers' instructions.

Statistics

Statistical analysis were performed using GraphPad Prism software (GraphPad Software, Inc.). Results are depicted as mean ± standard error of mean if not stated otherwise. For a two–group comparison, a t–test was applied if the pre–test for normality (D'Agostino–Pearson normality test) was not rejected at 0.05 significance level, otherwise a Mann–Whitney test for nonparametric data was used. For a comparison of more than two groups an ANOVA test, followed by a Bonferroni test for multiple comparison, was applied. For analysis of clinical data a Wilcoxon test for matched pairs was used. P values of < 0.05 indicate statistical significance.

Supplementary Material

Refer to Web version on PubMed Central for supplementary material.

Acknowledgments

The authors thank the CSB Mouse Imaging Program (Jessica Truelove, Derrick Jeon) for help with imaging, Miriam Stein, Irene Neudorfer and Fabian Meixner for help with the clinical study, Laura Prickett–Rice, Kathryn Folz–Donahue and Meredith Weglarz from the Flow Cytometry Core Facility (Massachusetts General Hospital, Center for Regenerative Medicine and Harvard Stem Cell Institute) and Michael Waring and Adam Chicoine from the Ragon Institute (of MGH, MIT and Harvard) for assistance with cell sorting. We are grateful to Drs. Paul Frenette, Bradford Lowell and Grigori Enikolopov for providing knock out or transgenic mice. We gratefully acknowledge the ICU team in Freiburg, Germany. This work was funded in part by grants from the US National Institute of Health R01–HL114477, R01–HL117829, R01–HL096576 (M.N.); HHSN268201000044C (R.W.). Timo Heidt and Hendrik B. Sager are funded by Deutsche Forschungsgemeinschaft (HE–6382/1–1 to TH and SA1668/2–1 to HBS).

REFERENCES

1. Black PH. The inflammatory response is an integral part of the stress response: Implications for atherosclerosis, insulin resistance, type II diabetes and metabolic syndrome X. Brain Behav Immun. 2003; 17:350–364. [PubMed: 12946657]
2. Rosengren A, et al. Association of psychosocial risk factors with risk of acute myocardial infarction in 11119 cases and 13648 controls from 52 countries (the INTERHEART study): case-control study. Lancet. 2004; 364:953–962. [PubMed: 15364186]
3. Glaser R, Kiecolt-Glaser JK. Stress-induced immune dysfunction: implications for health. Nat Rev Immunol. 2005; 5:243–251. [PubMed: 15738954]
4. Powell ND, et al. Social stress up-regulates inflammatory gene expression in the leukocyte transcriptome via beta-adrenergic induction of myelopoiesis. Proc Natl Acad Sci U S A. 2013; 110:16574–16579. [PubMed: 24062448]
5. Cohen S, Kamarck T, Mermelstein R. A global measure of perceived stress. J Health Soc Behav. 1983; 24:385–396. [PubMed: 6668417]
6. Lesage FX, Berjot S. Validity of occupational stress assessment using a visual analogue scale. Occup Med (Lond). 2011; 61:434–436. [PubMed: 21505089]
7. Schweizer MC, Henniger MS, Sillaber I. Chronic mild stress (CMS) in mice: of anhedonia, 'anomalous anxiolysis' and activity. PLoS One. 2009; 4:e4326. [PubMed: 19177164]
8. Nollet M, Guisquet AM, Belzung C. Models of depression: unpredictable chronic mild stress in mice. Curr Protoc Pharmacol. 2013 Chapter 5, Unit5.65.
9. Yalcin I, Aksu F, Belzung C. Effects of desipramine and tramadol in a chronic mild stress model in mice are altered by yohimbine but not by pindolol. Eur J Pharmacol. 2005; 514:165–174. [PubMed: 15910803]
10. Kiel MJ, et al. SLAM family receptors distinguish hematopoietic stem and progenitor cells and reveal endothelial niches for stem cells. Cell. 2005; 121:1109–1121. [PubMed: 15989959]
11. Wilson A, et al. Hematopoietic stem cells reversibly switch from dormancy to self-renewal during homeostasis and repair. Cell. 2008; 135:1118–1129. [PubMed: 19062086]
12. Szilvassy SJ, Humphries RK, Lansdorp PM, Eaves AC, Eaves CJ. Quantitative assay for totipotent reconstituting hematopoietic stem cells by a competitive repopulation strategy. Proc Natl Acad Sci U S A. 1990; 87:8736–8740. [PubMed: 2247442]
13. Essers MA, et al. IFNalpha activates dormant haematopoietic stem cells in vivo. Nature. 2009; 458:904–908. [PubMed: 19212321]
14. Baldridge MT, King KY, Boles NC, Weksberg DC, Goodell MA. Quiescent haematopoietic stem cells are activated by IFN-gamma in response to chronic infection. Nature. 2010; 465:793–797. [PubMed: 20535209]
15. Lo Celso C, Lin CP, Scadden DT. In vivo imaging of transplanted hematopoietic stem and progenitor cells in mouse calvarium bone marrow. Nat Protoc. 2011; 6:1–14. [PubMed: 21212779]

16. Mendez-Ferrer S, Lucas D, Battista M, Frenette PS. Haematopoietic stem cell release is regulated by circadian oscillations. Nature. 2008; 452:442–447. [PubMed: 18256599]
17. Spiegel A, et al. Catecholaminergic neurotransmitters regulate migration and repopulation of immature human CD34+ cells through Wnt signaling. Nat Immunol. 2007; 8:1123–1131. [PubMed: 17828268]
18. Lucas D, et al. Chemotherapy-induced bone marrow nerve injury impairs hematopoietic regeneration. Nat Med. 2013; 19:695–703. [PubMed: 23644514]
19. Zigmond RE, Ben-Ari Y. Electrical stimulation of preganglionic nerve increases tyrosine hydroxylase activity in sympathetic ganglia. Proc Natl Acad Sci U S A. 1977; 74:3078–3080. [PubMed: 19742]
20. Morrison SJ, Scadden DT. The bone marrow niche for haematopoietic stem cells. Nature. 2014; 505:327–334. [PubMed: 24429631]
21. Mendez-Ferrer S, et al. Mesenchymal and haematopoietic stem cells form a unique bone marrow niche. Nature. 2010; 466:829–834. [PubMed: 20703299]
22. Ding L, Morrison SJ. Haematopoietic stem cells and early lymphoid progenitors occupy distinct bone marrow niches. Nature. 2013; 495:231–235. [PubMed: 23434755]
23. Eash KJ, Means JM, White DW, Link DC. CXCR4 is a key regulator of neutrophil release from the bone marrow under basal and stress granulopoiesis conditions. Blood. 2009; 113:4711–4719. [PubMed: 19264920]
24. Tzeng YS, et al. Loss of Cxcl12/Sdf-1 in adult mice decreases the quiescent state of hematopoietic stem/progenitor cells and alters the pattern of hematopoietic regeneration after myelosuppression. Blood. 2011; 117:429–439. [PubMed: 20833981]
25. Nie Y, Han YC, Zou YR. CXCR4 is required for the quiescence of primitive hematopoietic cells. J Exp Med. 2008; 205:777–783. [PubMed: 18378795]
26. Libby P, Ridker PM, Hansson GK. Progress and challenges in translating the biology of atherosclerosis. Nature. 2011; 473:317–325. [PubMed: 21593864]
27. Randolph GJ. The fate of monocytes in atherosclerosis. J Thromb Haemost. 2009; 7(Suppl 1):28–30. [PubMed: 19630762]
28. Rader DJ, Daugherty A. Translating molecular discoveries into new therapies for atherosclerosis. Nature. 2008; 451:904–913. [PubMed: 18288179]
29. Swirski FK, Nahrendorf M. Leukocyte behavior in atherosclerosis, myocardial infarction, and heart failure. Science. 2013; 339:161–166. [PubMed: 23307733]
30. Moore KJ, Tabas I. Macrophages in the pathogenesis of atherosclerosis. Cell. 2011; 145:341–355. [PubMed: 21529710]
31. Libby P. Mechanisms of acute coronary syndromes and their implications for therapy. N Engl J Med. 2013; 368:2004–2013. [PubMed: 23697515]
32. Adamsson Eryd S, Smith JG, Melander O, Hedblad B, Engstrom G. Incidence of coronary events and case fatality rate in relation to blood lymphocyte and neutrophil counts. Arterioscler Thromb Vasc Biol. 2012; 32:533–539. [PubMed: 22116095]
33. Libby P. Inflammation in atherosclerosis. Nature. 2002; 420:868–874. [PubMed: 12490960]
34. Kaplan JR, et al. Social stress and atherosclerosis in normocholesterolemic monkeys. Science. 1983; 220:733–735. [PubMed: 6836311]
35. Gu H, Tang C, Peng K, Sun H, Yang Y. Effects of chronic mild stress on the development of atherosclerosis and expression of toll-like receptor 4 signaling pathway in adolescent apolipoprotein E knockout mice. J Biomed Biotechnol. 2009; 2009:613879. [PubMed: 19746160]
36. Bernberg E, Ulleryd MA, Johansson ME, Bergstrom GM. Social disruption stress increases IL-6 levels and accelerates atherosclerosis in ApoE-/- mice. Atherosclerosis. 2012; 221:359–365. [PubMed: 22284955]
37. Wilbert-Lampen U, et al. Cardiovascular events during World Cup soccer. N Engl J Med. 2008; 358:475–483. [PubMed: 18234752]
38. Wantha S, et al. Neutrophil-derived cathelicidin promotes adhesion of classical monocytes. Circ Res. 2013; 112:792–801. [PubMed: 23283724]

39. Weber C, Noels H. Atherosclerosis: current pathogenesis and therapeutic options. Nat Med. 2011; 17:1410–1422. [PubMed: 22064431]

40. Tall AR, Yvan-Charvet L, Westerterp M, Murphy AJ. Cholesterol efflux: a novel regulator of myelopoiesis and atherogenesis. Arterioscler Thromb Vasc Biol. 2012; 32:2547–2552. [PubMed: 23077140]

SUPPLEMENTARY REFERENCES

41. Purton LE, Scadden DT. Limiting factors in murine hematopoietic stem cell assays. Cell Stem Cell. 2007; 1:263–270. [PubMed: 18371361]

42. Hu Y, Smyth GK. ELDA: extreme limiting dilution analysis for comparing depleted and enriched populations in stem cell and other assays. J Immunol Methods. 2009; 347:70–78. [PubMed: 19567251]

43. Dutta P, et al. Myocardial infarction accelerates atherosclerosis. Nature. 2012; 487:325–329. [PubMed: 22763456]

44. Kobayashi M, Srour EF. Regulation of murine hematopoietic stem cell quiescence by Dmtf1. Blood. 2011; 118:6562–6571. [PubMed: 22039255]

45. Shi C, et al. Bone marrow mesenchymal stem and progenitor cells induce monocyte emigration in response to circulating toll-like receptor ligands. Immunity. 2011; 34:590–601. [PubMed: 21458307]

46. Westerterp M, et al. Regulation of hematopoietic stem and progenitor cell mobilization by cholesterol efflux pathways. Cell Stem Cell. 2012; 11:195–206. [PubMed: 22862945]

47. Schepers K, et al. Myeloproliferative neoplasia remodels the endosteal bone marrow niche into a self-reinforcing leukemic niche. Cell Stem Cell. 2013; 13:285–299. [PubMed: 23850243]

48. Seimon TA, et al. Macrophage deficiency of p38alpha MAPK promotes apoptosis and plaque necrosis in advanced atherosclerotic lesions in mice. J Clin Invest. 2009; 119:886–898. [PubMed: 19287091]

49. Zaheer A, et al. In vivo near-infrared fluorescence imaging of osteoblastic activity. Nat Biotechnol. 2001; 19:1148–1154. [PubMed: 11731784]

50. Nahrendorf M, et al. Hybrid PET-optical imaging using targeted probes. Proc Natl Acad Sci U S A. 2010; 107:7910–7915. [PubMed: 20385821]

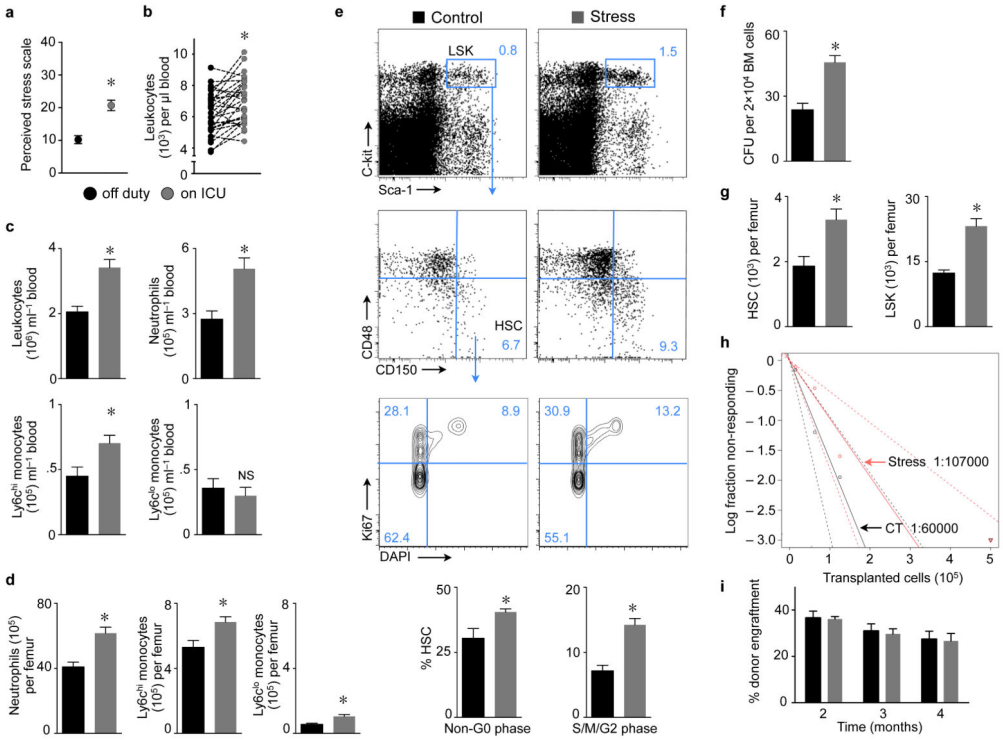

Figure 1. Chronic stress increases proliferation of hematopoietic stem and progenitor cells in the bone marrow

a, Cohen's perceived stress scale score in medical ICU residents (n = 10–15, Student's t–test). **b**, Blood leukocytes in residents (*n* = 29, Wilcoxon test). **c**, Leukocytes in mouse blood and **d,** bone marrow after 3 weeks of stress (*n* = 9 per group, Student's t–test). **e,** Gating for LSK and HSC. Proliferation was assessed after 3 weeks of stress (*n* = 5 per group, Mann–Whitney test). **f,** Bone marrow colony forming unit (CFU) assay after one week of stress (*n* = 5 per group, Mann–Whitney test). **g,** Bone marrow HSC and LSK after 3 weeks of stress (*n* = 10 per group, Student's t–test). **h,** Long–term competitive repopulation assay using limiting dilutions of whole bone marrow from stressed or non–stressed mice (Poisson statistics for LT–HSC frequencies, $P = 0.2$ two–tailed t–test). **i,** Competitive reconstitution with 2×10^6 bone marrow cells from stressed or non–stressed controls co–injected with equal numbers of naive competitor cells, followed by assessment of blood chimerism (*n* = 10 mice per group, one–way ANOVA). Mean ± s.e.m., * $P < 0.05$.

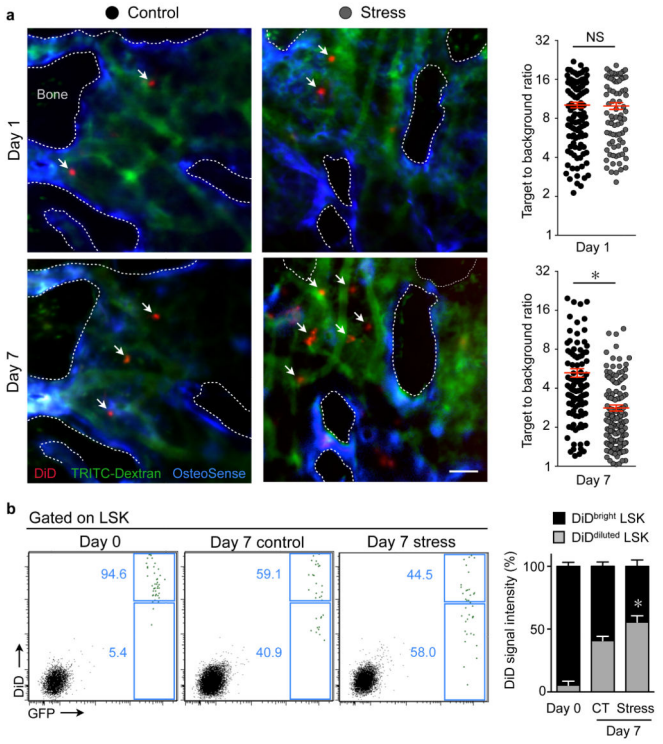

Figure 2. Hematopoietic progenitors in the bone marrow of stressed mice dilute DiD membrane dye faster

a, Intravital microscopy of the mouse calvarium after adoptive transfer of DiD–labelled LSK (white arrows) before and seven days after stress (n = 5 mice per group, Mann–Whitney test). Dotted lines outline bone. Scale bar indicates 50 μm. Single dots in graphs represent DiD^+ cells' target–to–background ratio before (upper panel) and after stress (lower panel). **b,** DiD fluorescence on day 0 and 7 days after adoptive transfer of DiD^+ GFP^+ LSK in non–stressed control (CT) or stressed mice (n = 5 per group). The bar graph illustrates the DiD fluorescence in GFP^+ LSK (Mann–Whitney test). Mean ± s.e.m., * $P < 0.05$.

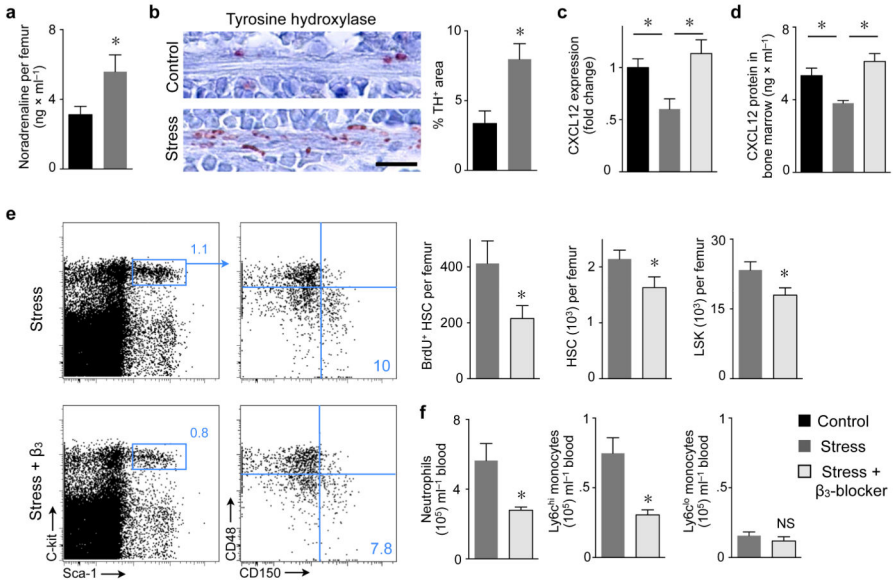

Figure 3. Stress–induced sympathetic nervous signaling regulates proliferation of bone marrow HSC via CXCL12

a, Noradrenaline ELISA after 3 weeks of stress (*n* = 8 per group, Student's t–test). **b,** Immunoreactive staining for tyrosine hydroxylase (TH) in bone marrow. Scale bar indicates 10 μm. Bar graph shows TH–positive area (*n* = 5 mice per group, Mann–Whitney test). **c,** CXCL12 mRNA in bone marrow (*n* = 10 per group, one–way ANOVA). **d,** CXCL12 protein in bone marrow (*n* = 7 per group, one–way ANOVA). **e,** Dot plots and quantification of LSK and HSC (*n* = 5 per group, Mann–Whitney test). **f,** Effects of β_3 adrenoreceptor blocker on blood leukocytes (*n* = 5 per group, Mann–Whitney test). Mean ± s.e.m., * $P < 0.05$.

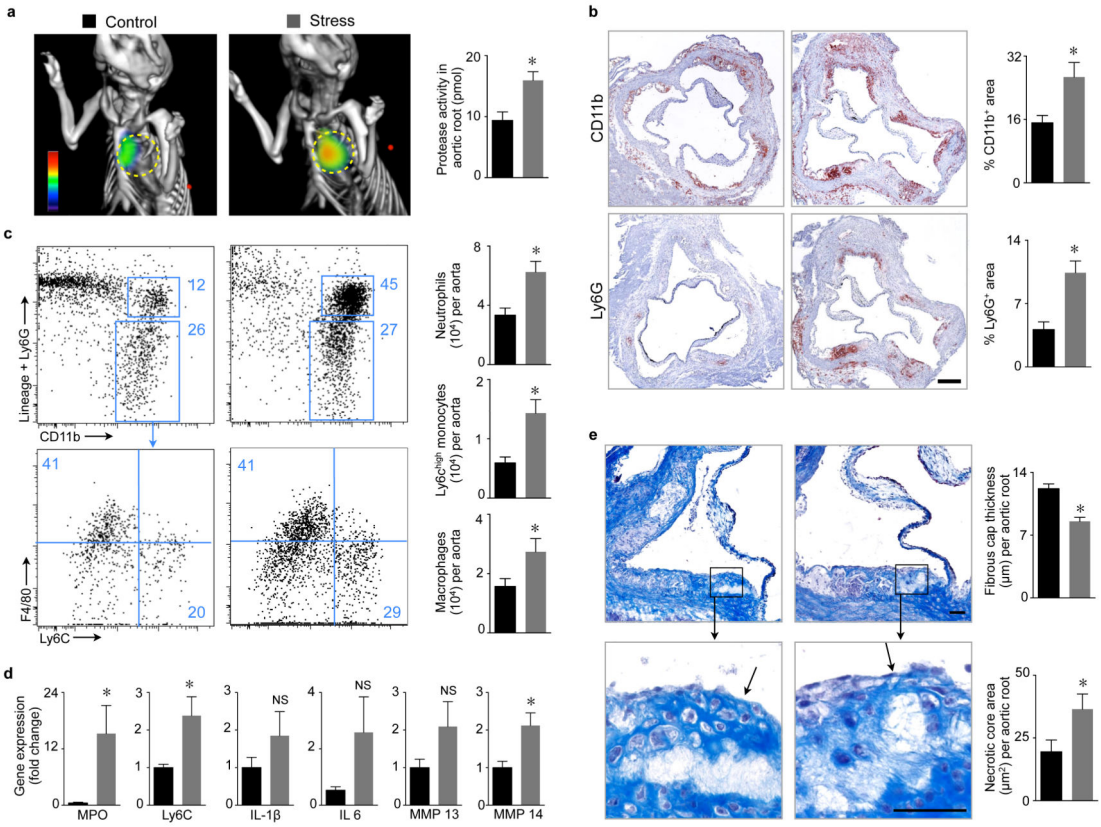

Figure 4. Chronic stress increases inflammation in mouse atherosclerotic plaques

a, Protease activity in aortic roots of *ApoE*$^{-/-}$ mice measured by FMT–CT after 6 weeks of stress. Circles indicate aortic root (n = 5 per group, Mann–Whitney test). **b,** Immunoreactive staining of aortic roots for CD11b and Ly6G. Bar graphs show percentage of positive area per root (n = 9–10 per group, Student's t–test). Scale bar indicates 200 μm. **c,** Gating and quantification of aortic myeloid cells (n = 10 per group, Student's t–test). **d,** qPCR for inflammatory genes in aorta (n = 9–10 per group, Student's t–test). **e,** Masson trichrome staining (n = 9 per group, Student's t–test). Scale bar indicates 50 μm, arrows point at fibrous cap covering necrotic core. Bar graphs show fibrous cap thickness and necrotic core area. Mean ± s.e.m., *P < 0.05.